EXTENDED SUPPORT MATERIALS

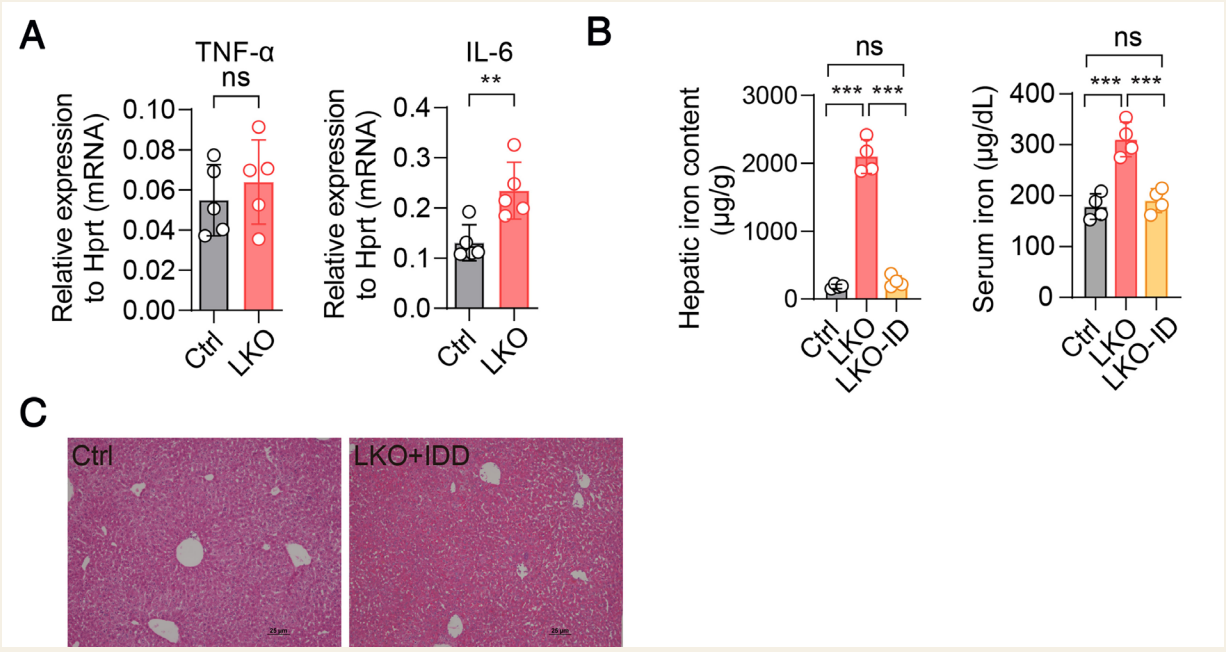

Extended Support Figure 1. Iron overload was not the major factor for the susceptible of LKO mice to bacterial infection.

(A) The mRNA level of TNF-α and IL-6 in the liver of control (n = 5) and LKO mice (n = 5) 12 h post *E. coli* infection; (B) The iron level in the liver and serum of Control, LKO and LKO + ID mice (n = 4); (C) Representative hematoxylin and eosin staining of histological sections of liver tissue in control and LKO + ID mice 12 h post infection. Circles correspond to individual mouse. Results are represented as mean ± SD. P values in (A) were determined using unpaired Student's t-tests. P values in (B) were determined using one-way ANOVA. $^{*}P < 0.05$; $^{**}P < 0.01$; $^{***}P < 0.001$. NS: Not significant; TNF-α: tumor necrosis factor-alpha; IL-6: interleukin-6; LKO: liver-specific Smad4 knockout; *E. coli: Escherichia coli.*

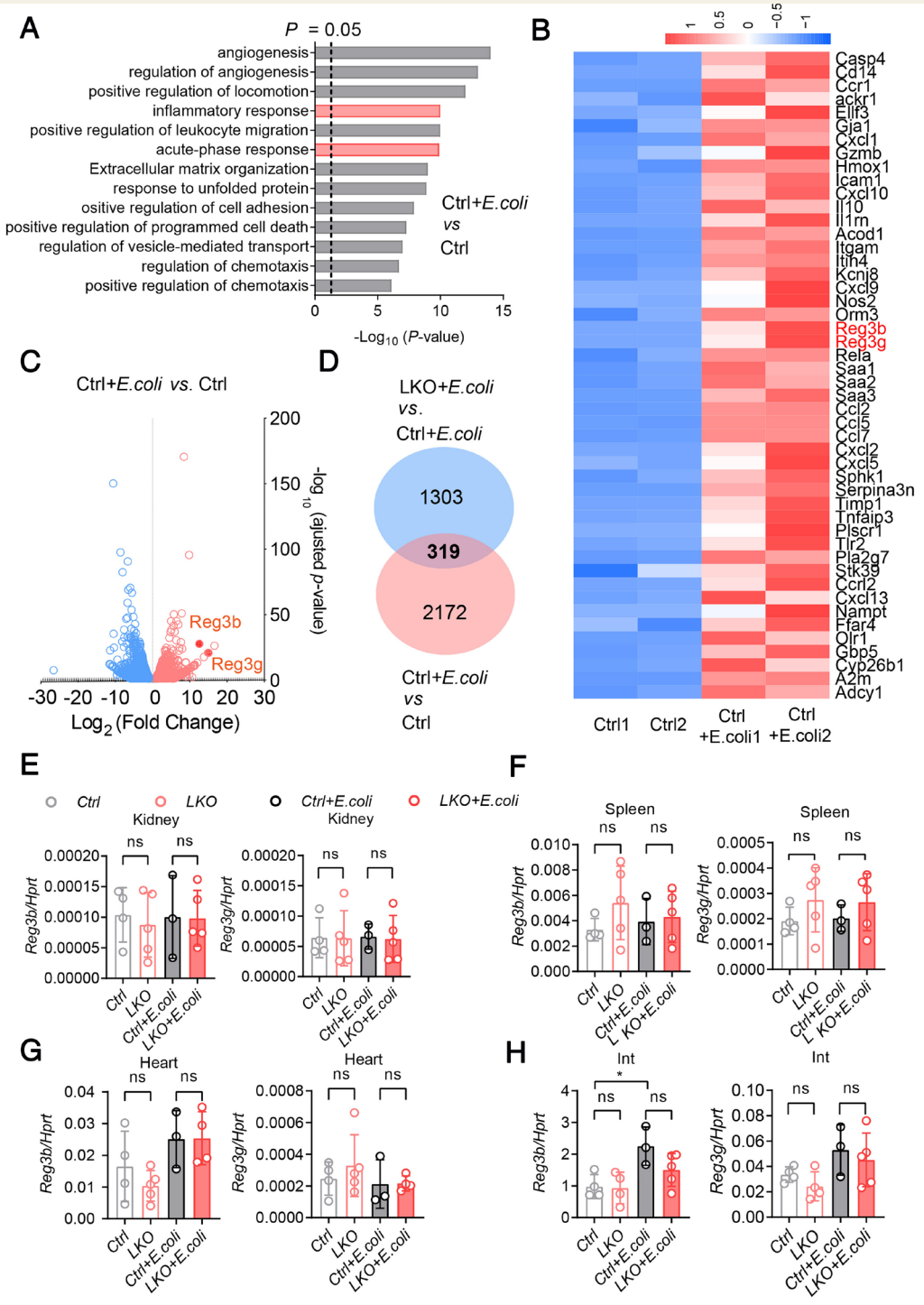

Extended Support Figure 2. The expression of *Reg3b* and *Reg3g* is upregulated upon *E. coli* infection.
(A) Go analysis of differentially expressed genes (upregulated) in the liver from Ctrl + *E. coli* and Ctrl mice; (B) Heat map representation of differentially upregulated genes in the inflammatory response pathway (Ctrl + *E. coli* group *vs.* Ctrl group); (C) Volcano plot representation of RNA sequencing data of genes upregulated (red) or downregulated (blue) in the liver from Ctrl + *E. coli* and Ctrl mice; (D) The venn diagram showing the number of differentiated expressed genes in LKO + *E. coli vs.* Ctrl + *E. coli* group and Ctrl + *E. coli vs.* Ctrl group; (E) The mRNA level of *Reg3b* and *Reg3g* in the kidney of control and LKO mice (non-infected and 12 h post *E. coli* infection, respectively) (n = 3-5 per group); (F) The mRNA level of *Reg3b* and *Reg3g* in the spleen of control and LKO mice (non-infected and 12 h post *E. coli* infection, respectively) (n = 3-5 per group); (G) The mRNA level of *Reg3b* and *Reg3g* in the heart of control and LKO mice (non-infected and 12 h post *E. coli* infection, respectively) (n = 3-5 per group); (H) The mRNA level of *Reg3b* and *Reg3g* in the intestine of control and LKO mice (non-infected and 12 h post *E. coli* infection, respectively) (n = 3-5 per group). Circles correspond to individual mouse. Results are represented as mean ± SD. The P values in (C) were deter-mined using unpaired Student's t-tests. $^{*}P < 0.05$; $^{**}P < 0.01$; $^{***}P < 0.001$. LKO: Liver-specific Smad4 knockout; *E. coli*: *Escherichia coli*.

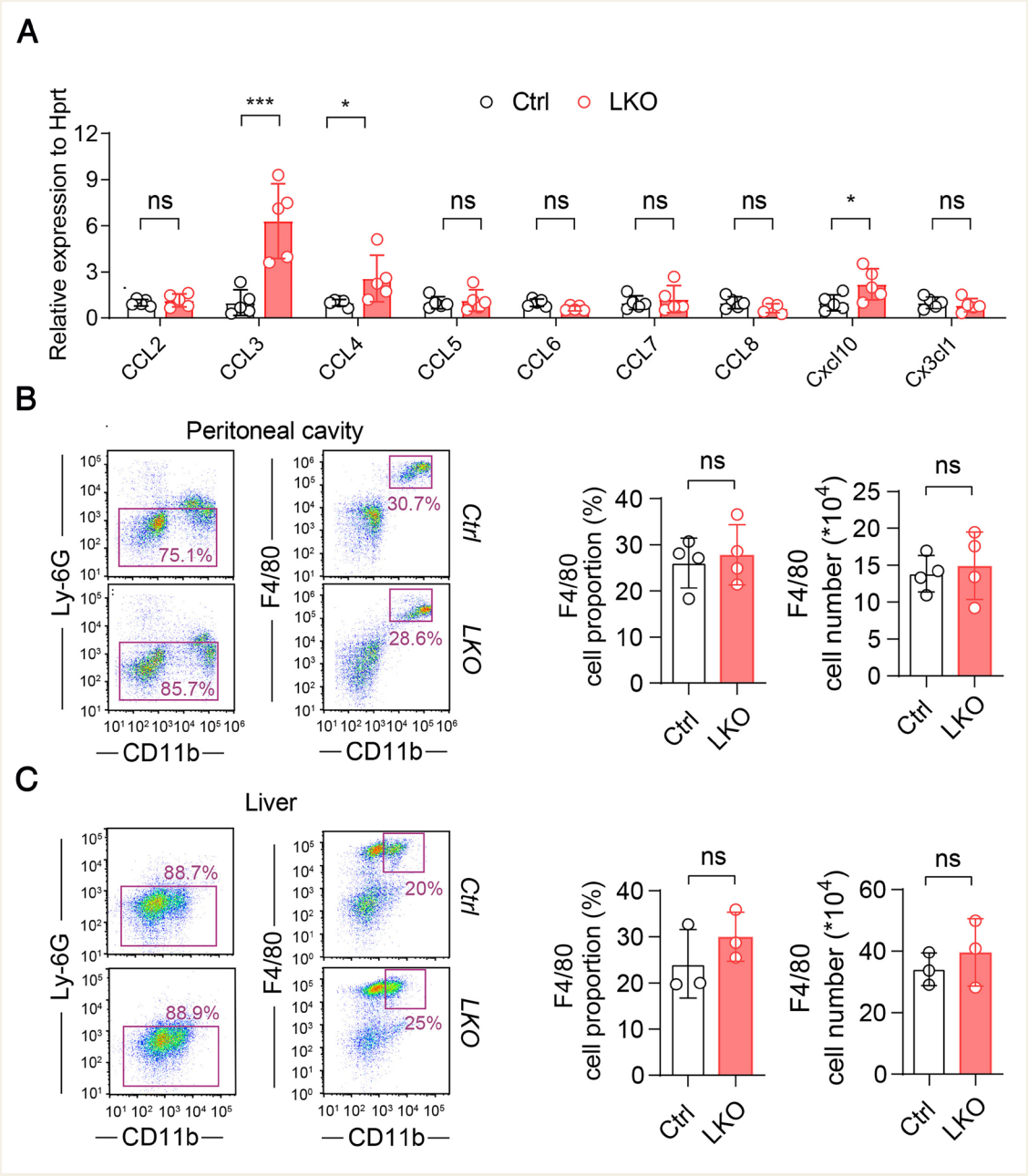

Extended Support Figure 3. Hepatic Smad4 deficiency do not affect the number of macrophages at non-infected conditions.
(A) The mRNA levels of several chemokines (*Ccl2, Ccl3, Ccl4, Ccl5, Ccl6, Ccl7, Ccl8, Cxcl10, Cx3cl1*; quantified by RT-PCR) in the liver of control (n = 5) and LKO mice (n = 5) 12 h post *E. coli* infection; (B) Representative flow cytometry dot plot and corresponding proportion and cell number of macrophages in the peritoneal fluid from control (n = 4) and LKO (n = 4) mice; (C) Representative flow cytometry dot plot and corresponding proportion and cell number of macrophages in the liver from control (n = 3) and LKO (n = 3) mice. Circles correspond to individual mouse. Results are represented as mean ± SD and are obtained at embryonic day 16.5. The P values in (A-C) were determined using unpaired Student's t-tests. $^{*}P < 0.05$; $^{**}P < 0.01$; $^{***}P < 0.001$. NS: not significant; LKO: liver-specific Smad4 knockout; *E. coli*: *Escherichia coli.*

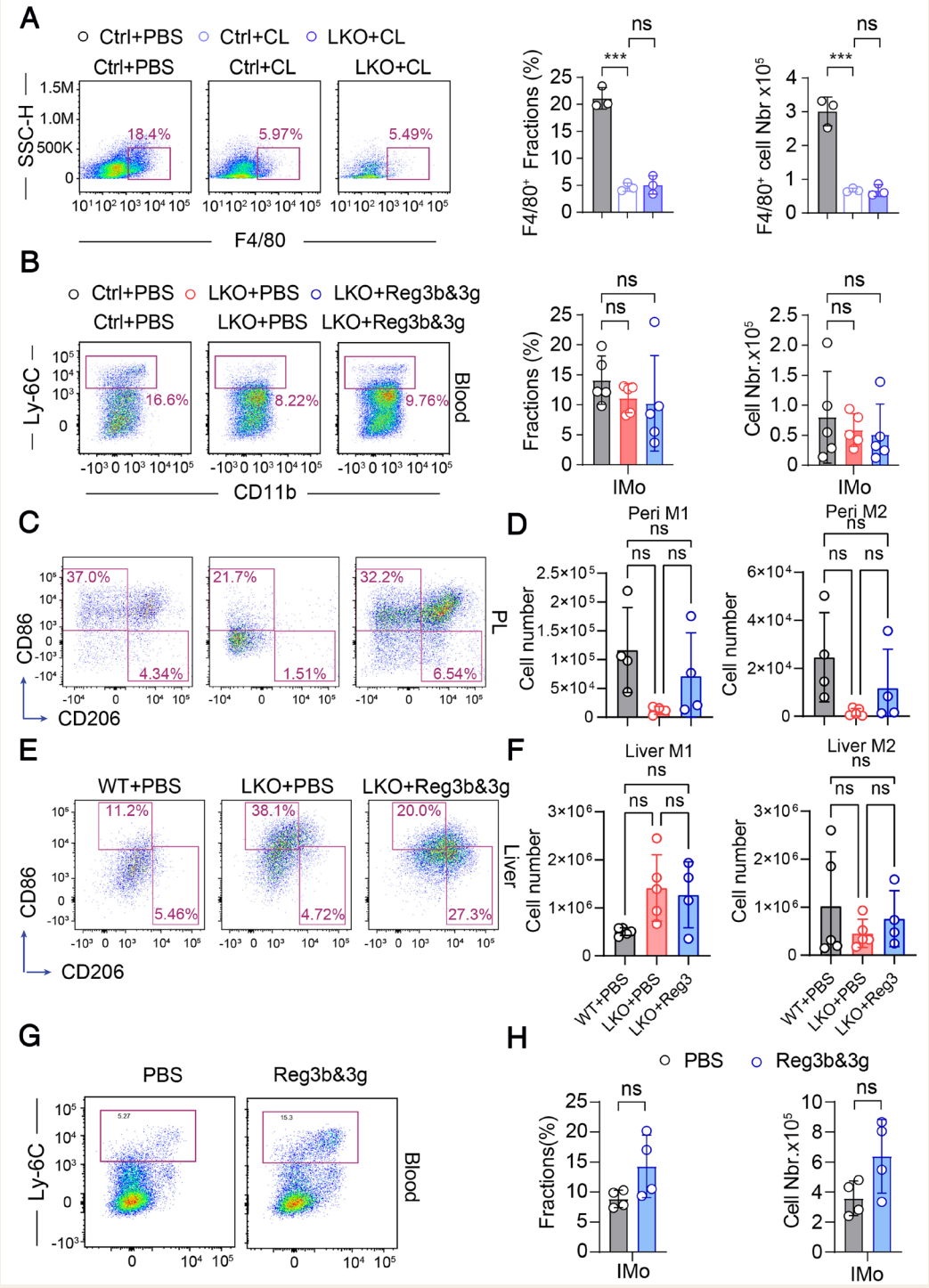

Extended Support Figure 4. *Reg3b* and *Reg3g* exert anti-bacterial activity through recruitment of macrophages.
(A) Representative flow cytometry dot plot and corresponding proportion and cell number of F4/80$^+$ cells in the peritoneal fluid from control, LKO + PBS and LKO + clodronate liposomes mice 48 h post infection; (B) Representative flow cytometry dot plot and corresponding propor-tion and cell number of inflammatory monocytes in the blood from control, LKO + PBS, LKO + rReg3b and rReg3g mice; (C) The corresponding flow cytometry dot plot and cell number of M1 and M2 macrophages in the peritoneal fluid of control, LKO + PBS and LKO + rReg3b and rReg3g mice (n = 4-5 per group); (D) The corresponding flow cytometry dot plot and cell number of M1 and M2 macrophages in the liver of control, LKO + PBS and LKO + rReg3b and rReg3g mice (n = 4-5 per group); (E) Representative flow cytometry dot plot of monocytes in the blood and liv-er of WT + PBS and WT + rReg3b and rReg3g mice; (F) The cell number of inflammatory monocytes in the blood of WT + PBS and WT + rReg3b and rReg3g mice. Circles correspond to individual mouse. Results are represented as mean ± SD. The P values in (A and B) were determined us-ing one-way ANOVA. The P values in (D-F) were determined using unpaired Student's t -tests. The P values in (E) were determined using two-way ANOVA. $^*P < 0.05$; $^{**}P < 0.01$; $^{***}P < 0.001$. LKO: Liver-specific Smad4 knockout; PBS: phosphate buffered saline; WT: wild type.

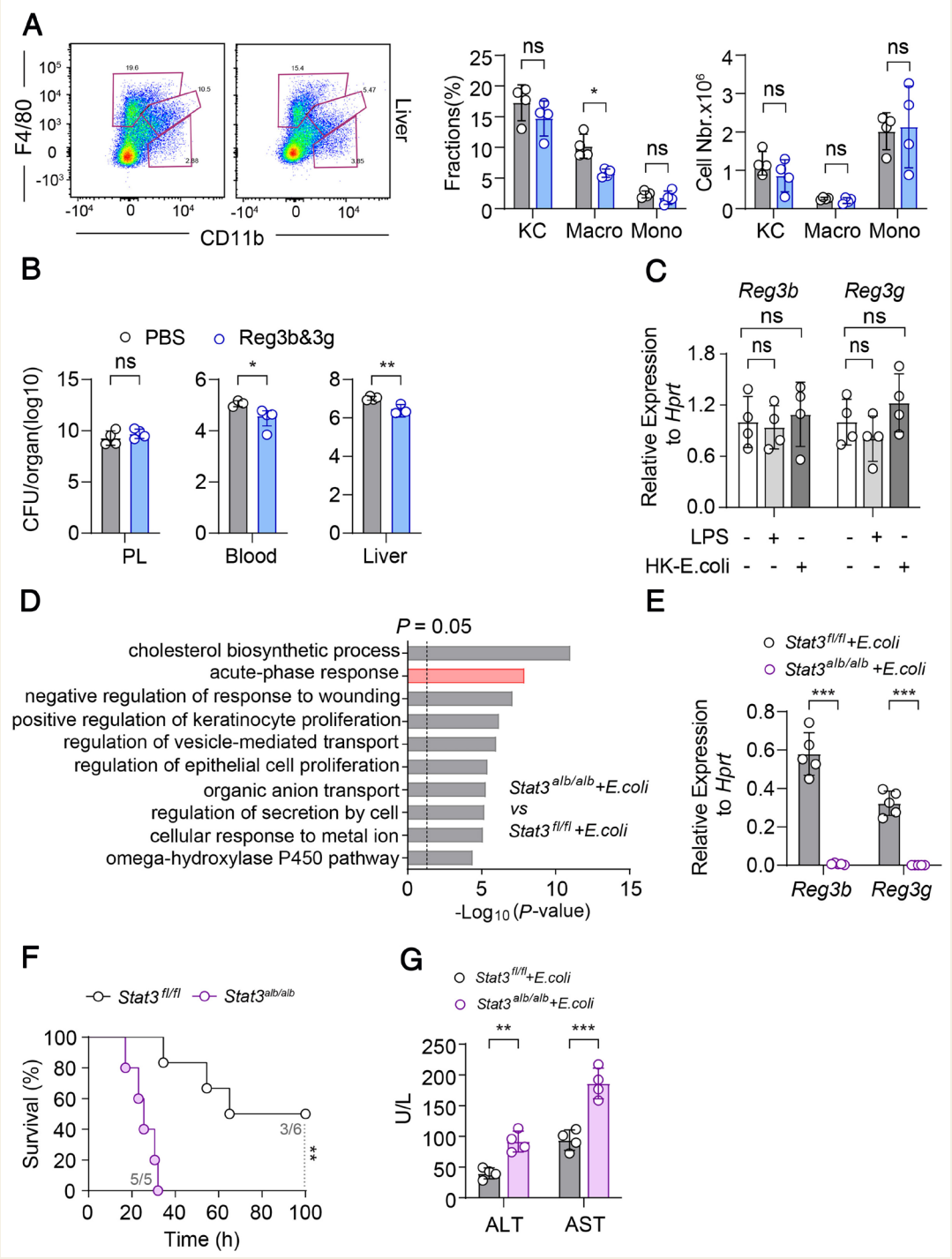

Extended Support Figure 5. Hepatic stat3 deficiency resulted in decreased *Reg3b* and *Reg3g* expression upon infection.
(A) The corresponding proportion and cell number of immnue cells (kuffer cells, macrphages and monocytes) in the liver of WT + PBS and WT + rReg3b and rReg3g mice; (B) The bacterial CFU counts measured in the peritoneal fluid, blood and liver of WT + PBS and WT + rReg3b and rReg3g mice 12 h post infection; (C) The mRNA levels of *Reg3b* and *Reg3g* measured in primary hepatocytes isolated from control and LKO mice and treated with LPS or heat-killed *E. coli* (HK-*E. coli*); (D)Go analysis of differentially expressed genes (downregulated) in the liver from $Stat3^{fl/fl}$ and $Stat3^{fl/fl}$; Alb-cre ($Stat3^{alb/alb}$) mice 12 h post infection; (E) The mRNA level of *Reg3b* and *Reg3g* in the liver of $Stat3^{fl/fl}$ (n = 5) and $Stat3^{alb/alb}$ mice (n = 5) 12 h post infection; (F) Kaplan-Meier survival curve of $Stat3^{alb/alb}$ mice (n = 5) and $Stat3^{fl/fl}$ mice (n = 6) following an i.p. injection of *E. coli*; (G) Serum ALT and AST levels of $Stat3^{fl/fl}$ (n = 4) and $Stat3^{alb/alb}$ mice (n = 4) were measured 12 h post infection. Circles correspond to individual mouse. Results are represented as mean ± SD. P values in (A) were determined using one-way ANOVA. P values in (C) were determined using unpaired Student's t-tests. $^{*}P < 0.05$; $^{**}P < 0.01$; $^{***}P < 0.001$. NS: Not significant; LKO: liver-specific Smad4 knockout; PBS: phosphate buffered saline; WT: wild type; CFU: colony forming unit; LPS: lipopolysaccharide; ALT: alanine aminotransferase; AST: as-partate aminotransferase; *E. coli: Escherichia coli.*

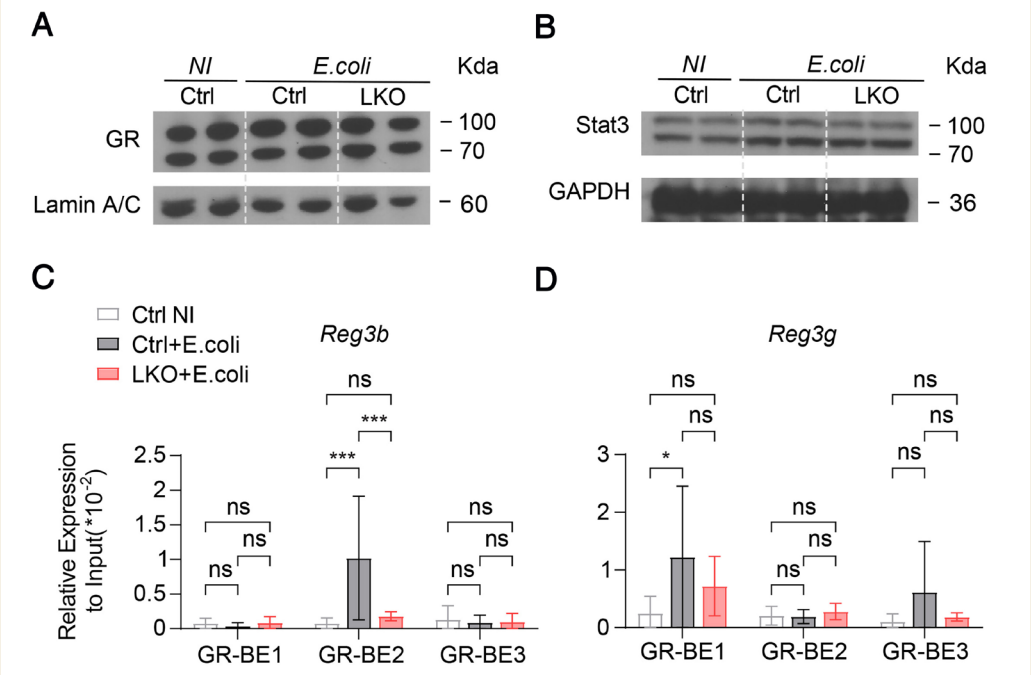

Extended Support Figure 6. Smad4 regulated the expression of *Reg3b* and *Reg3g* via GR.
(A) Western blot analysis of Stat3 protein in the liver tissues of non-infected control mice, *E. coli* infected control mice and *E. coli* infected LKO mice; (B) Western blot analysis of Glucocorticoid Receptor protein in the liver tissues of non-infected control mice, *E. coli* infected con-trol mice and *E. coli* infected LKO mice; (C) ChIP assay using GR antibody followed by qPCR of the *Reg3b* promoter (GR-BE1, GR-BE2) in the liver of non-infected control mice, *E. coli* infected control mice and *E. coli* infected LKO mice; (D) ChIP assay using GR antibody followed by qPCR of the Reg3g promoter (GR-BE1, GR-BE2) in the liver of non-infected control mice, *E. coli* infected control mice and *E. coli* infected LKO mice. Circles correspond to individual mouse. Results are represented as mean ± SD. The P values in (C and D) were determined using one-way ANOVA. $^{*}P < 0.05$; $^{**}P < 0.01$; $^{***}P < 0.001$. NS: not significant; ChIP: chromatin immunoprecipitation; GR: glucocorticoid receptor; qPCR: quantitative polymerase chain reaction; LKO: liver-specific Smad4 knockout; *E. coli*: *Escherichia coli*.

Extended Support Table 1. Sequences of the primers used for genotyping PCR analyses

Gene	Forward primers	Reverse primers
Smad4	GGGCAGCGTAGCATATAAGA	GACCCAAACGTCACCTTCAG
Alb-cre	GCAAACATACGCAAGGGATT	AGGCAAATTTTGGTGTACGG

Extended Support Table 2. Sequences of the primers used for ChIP analysis of the mouse *Reg3b* promoter

Gene	Forward primers	Reverse primers
mReg3b-Smad4-1	AAAGCAAGAAAGTAATCCCTCA	AGGAAAAGTAATTGTTGCTTCGTA
mReg3b-Smad4-2	ACACCTACAATTTTTAATCTGCTCA	TCAATTTGGAAAAACCTCACTTGT
mReg3b-Stat3-1	AGGTAAAGCAGGTCGGCTAA	TGAGGGAGGGACATCGTAGTA
mReg3b-Stat3-2	AATTTGTGCCCCAATGTTGCC	TTAGCCGACCTGCTTTACCTC
mReg3b-GR-1	CCCAATGTTGCCATTGTTTGC	TTAGCCGACCTGCTTTACCTC
mReg3b-GR-2	GTAAAGCAGGTCGGCTAACG	CAGCATTTGGCACAGACTCAA
mReg3b-GR-3	AGGTAAAGCAGGTCGGCTAA	AGCATTTGGCACAGACTCAA

ChIP: Chromatin immunoprecipitation.

Extended Support Table 3. Sequences of the primers used for ChIP analysis of the mouse *Reg3g* promoter

Gene	Forward primers	Reverse primers
mReg3g-Smad4-1	GAGGATGTGCCTAATCCTATAGG	ACCCAGACTCTCTCCCTCATT
mReg3g-Smad4-2	GAAACGTGAACTCCTTTCTGCC	GTGTGCTTTAGCATTAATCCATCC
mReg3g-Smad4-3	ATGAAAACTACGTCAAAGCCATTC	TGCCTCTCTGTGGGAAAGTTG
mReg3g-Stat3-1	GAGGCAGCAGGAAAGCAAGT	TGATGGTCGTGAATTAGCTGAAAG
mReg3g-Stat3-2	GCATTGTGACAAAAATACCCTGTTA	TTGAACTTTCCCCATCTTTTCCC
mReg3g-Stat3-3	CTGCTAACAGGAAAGGGCCA	TGCTCATGCAAGTCAGGGAG
mReg3g-GR-1	TGGCATCCTTAGAGCTTCAGAG	AGGTGTTAAAGTGCTGAGGTACA
mReg3g-GR-2	GCATCCTTAGAGCTTCAGAGAC	TGTCCCCAACTTAAAAGAGTCA
mReg3g-GR-3	ACAGGCAGAATGTATGGAAGGAA	TGCCACAATCCAAACCTGTCT

ChIP: Chromatin immunoprecipitation.

Extended Support Table 4. Sequences of the primers used for RT-PCR and plasmid construction

Gene	Primers for RT-PCR	Reference
Hprt-F	TTTCCCTGGTTAAGCAGTACAGCCC	Nomura *et al.*, 2016[69]
Hprt-R	TGGCCTGTATCCAACACTTCGAGA	
Gapdh-F	ATCATCCCTGCATCCACT	Adedoyin *et al.*, 2018[70]
Gapdh-R	ATCCACGACGGACACATT	
Reg3b-F	GAGGCCTGGAGGACACCTCGT	Lörchner *et al.*, 2015[71]
Reg3b-R	TTGTCCCTTGTCCATGATGCTCTTC	
Reg3g-F	TTCCTGTCCTCCATGATCAAAA	Ito *et al.*, 2017[72]
Reg3g-R	CATCCACCTCTGTTGGGTTCA	
TNF-α-F	GGCAGGTCTACTTTGGAGTCATTGC	Dube *et al.*, 2001[73]
TNF-α-R	ACATTCGAGGCTCCAGTGAATTCGG	
Il6-F	CTGGTGACAACCACGGCCTTCCCTA	Liu *et al.*, 2006[74]
Il6-R	ATGCTTAGGCATAACGCACTAGGTT	
CCl2-F	CACCTGCTGCTACTCATTCAC	Huang *et al.*, 2007[75]
CCl2-R	CACTGTCACACTGGTCACTCCTAC	
CCl3-F	TGAATGCCTGAGAGTCTTGG	Ma *et al.*, 2021[76]
CCl3-R	TTGGCAGCAAACAGCTTATC	
CCl4-F	TCTGCGTGTCTGCCCTCTC	Fine *et al.*, 2003[77]
CCl4-R	TGCTGAGAACCCTGGAGCA	
CCl5-F	GTTATGGGAGGGCTCTGGTG	Fine *et al.*, 2003[77]
CCl5-R	CCTAAGCACCAGCTCTGCG	
CCl7-F	GCGTGCATCATTGAGAAAGGA	Lee *et al.*, 2009[78]
CCl7-R	ATGGCAGTGCTCTGTGATGT	
CCl8-F	GCTACGAGAGAATCAACAATATCCAGT	Marinkovic *et al.*, 2006[79]
CCl8-R	CAGAGAGACATACCCTGCTTGGT	
Cxcl10-F	GGAGATGAGCTAGGATAGGATAGAGGG	Makuch *et al.*, 2022[80]
Cxcl10-R	TGCCCATTTTCCCAGGACCG	
Cx3cl1-F	ACGAAATGCGAAATCATGTGC	Liu *et al.*, 2025[81]
Cx3cl1-R	CTGTGTCGTCTCCAGGACAA	

Extended Support Table 5. Antibody and fluorescent labels used for FACS sorting and analysis

Antigen	Fluorochrome	Company	Clone	Catalog
CD45	BV750	Biolegend	30-F11	103157
F4/80	BV605	Biolegend	BM8	123133
CD11b	APC-CY7	Elabscience	M1/70	E-AB-F1081S
Ly-6C	APC	Elabscience	Monts 1	E-AB-F1121E
Ly-6G	PerCP-Cy5.5	Elabscience	1A8	E-AB-F1108J
LD	Amcyan	Biolegend	D7	423101
CD16/32	PerCP-Cy5.5	Biolegend	93	101302

EXTENDED SUPPORT REFERENCES

69. Nomura, M.; et al. Fatty acid oxidation in macrophage polarization. *Nat. Immunol.* **17**, 216-217 (2016). https://doi.org/10.1038/ni.3366
70. Adedoyin, O.; et al. Heme oxygenase-1 mitigates ferroptosis in renal proximal tubule cells. *Am. J. Physiol. Renal Physiol.* **314**, F702-14 (2018). https://doi.org/10.1152/ajprenal.00044.2017
71. Lörchner, H.; et al. Myocardial healing requires Reg3β-dependent accumulation of macrophages in the ischemic heart. *Nat. Med.* **21**, 353-62 (2015). https://doi.org/10.1038/nm.3816
72. Ito, T. ;et al. Il-22 induces reg3γ and inhibits allergic inflammation in house dust mite-induced asthma models. *J Exp. Med.* **214**, 3037-50 (2017). https://doi.org/10.1084/jem.20162108
73. Dube, P. H.; Revell, P. A.; Chaplin, D. D.; Lorenz, R. G.; Miller, V. L. A role for Il-1 alpha in inducing pathologic inflammation during bacterial infection. *Proc Natl. Acad Sci U S A.* **98**, 10880-5 (2001). https://doi.org/10.1073/pnas.191214498
74. Liu, D. F.; Wei, W.; Song, L. H. Upregulation of TNF-alpha and Il-6 mrna in mouse liver induced by bacille Calmette-Guerin plus lipopolysaccharide. *Acta. Pharmacol. Sin.* **27**, 460-8 (2006). https://doi.org/10.1111/j.1745-7254.2006.00301.x
75. Huang, B.; et al. CCL2/CCR2 pathway mediates recruitment of myeloid suppressor cells to cancers. *Cancer Lett.* **252**, 86-92 (2007). https://doi.org/10.1016/j.canlet.2006.12.012
76. Ma, D.; Qiao, L.; Guo, B. Smad7 suppresses melanoma lung metastasis by impairing Tregs migration to the tumor microenvironment. *Am. J. Transl. Res.* **13**, 719-31 (2021). https://pubmed.ncbi.nlm.nih.gov/33594321/
77. Fine, J. S.; et al. Impairment of leukocyte trafficking in a murine pleuritis model by IL-4 and IL-10. *Inflammation.* **27**, 161-74 (2003). https://doi.org/10.1023/a:1025076111950
78. Lee, H. S.; Park, J. H.; Kang, J. H.; Kawada, T.; Yu, R.; Han, I. S. Chemokine and chemokine receptor gene expression in the mesenteric adipose tissue of KKAy mice. *Cytokine.* **46**, 160-5. (2009). https://doi.org/10.1016/j.cyto.2008.12.025
79. Marinkovic, T.; et al. Interaction of mature $CD3^{+}CD4^{+}$ T cells with dendritic cells triggers the development of tertiary lymphoid structures in the thyroid. *J. Clin. Invest.* **116**, 2622-32 (2006). https://doi.org/10.1172/jci28993
80. Makuch, E.; Jasyk, I.; Kula, A.; Lipiński, T.; Siednienko, J. IFNβ-induced CXCL10 chemokine expression is regulated by pellino3 ligase in monocytes and macrophages. International journal of molecular sciences. **23**, 14915 (2022). https://doi.org/10.3390/ijms232314915
81. Liu, P. P.; et al. Neuronal cathepsin S increases neuroinflammation and causes cognitive decline via CX3CL1-CX3CR1 axis and JAK2-STAT3 pathway in aging and Alzheimer's disease. *Aging Cell.* **24**, e14393 (2025). https://doi.org/10.1111/acel.14393